Hindawi
Scientific Programming
Volume 2021, Article ID 3739045, 9 pages
https://doi.org/10.1155/2021/3739045

Research Article

Psychological Stress Detection and Early Warning System Based on Wireless Network Transmission

Yaling Li

Shenzhen Technology University, Shenzhen, Guangdong 518118, China

Correspondence should be addressed to Yaling Li; liyaling@sztu.edu.cn

Received 16 June 2021; Revised 21 July 2021; Accepted 3 August 2021; Published 12 August 2021

Academic Editor: Mian Ahmad Jan

To improve the accuracy of stress detection and stress warning errors, this paper designed a new psychological stress detection and warning system based on wireless network transmission. To achieve this objective, we established a real-time setup. The hardware of the system is composed of pulse acquisition module, signal low-pass filtering and amplification module, real-time clock module, wireless network transmission module, and power supply module, respectively. Based on the aforementioned hardware platform, the system software is designed, mainly through the construction of pulse signal noise and the use of wavelet denoising threshold for sensing wavelet packet inverse transformation, to get the reconstructed signal. The peak point of the reconstructed signal is determined, and the value of pulse signal is extracted. According to the characteristic value's extraction results, the degree of psychological stress is quantified using the psychological stress index (PSI). When the PSI exceeds a predefined threshold, it indicates an early warning of psychological stress. The experimental results show that the psychological stress detection of our system is consistent with the expert evaluation results, the warning time is short, and the practical application effect is good.

1. Introduction

Psychological stress is an important factor affecting human health. It is composed of multiple components such as cognition, psychology, and behavior and is a complex response mode, which is manifested as a person's physical and psychological tension when facing difficult requirements or environment [1]. According to research findings, a certain degree of psychological pressure (benign pressure) can stimulate people's initiative and improve productivity, but excessive psychological pressure will bring a series of problems. Under excessive psychological pressure, people's decision-making perception ability is affected, which damages productivity [2]. Long-term psychological pressure causes diseases like cerebrovascular disease, cardiovascular disease, and immune deficiency along with mental illness such as depression and anxiety. Hence, a person's life and health are impacted, which makes him/her unable to withstand the psychological pressure caused by social security incidents [3]. Therefore, the diagnosis and research of psychological stress are of great significance to human health and social stability [4].

Psychological stress is an important factor affecting human health. When psychological stress exceeds the bearing ability of an individual, it leads to a high incidence of diseases and affects human health [5]. In real life, psychological pressure has increasingly become a major factor affecting people's physical and mental health and quality of life [6]. For effective detection and warning of psychological stress, quantitative measurement is required. However, subjective emotions and outsiders' experience cannot accurately evaluate a person's psychological stress, and the judgment must be assisted by the body's signs, so as to improve the effect of psychological stress detection and warning [7].

Therefore, according to the above analysis, this paper designed a psychological stress detection and early warning system based on wireless network transmission. The major contributions of this work are as follows:

(1) This paper provides real-time measurement for psychological stress by designing an early warning system. The hardware design platform is discussed in

detail and its distinguishing features are highlighted. To this end, this paper discusses its own unique wireless network transmission module.

(2) Pulse signal's noise is examined and a low-pass filter is used to protect the voiceless component in the speech signal. The low-pass filters smooth the TEO coefficient by obtaining a mask for a particular subband. Using the coefficient and masking, the inverse wavelet packet transform of perception is carried out to obtain the reconstructed signal.

The rest of this paper is organized as follows. In Section 2, the psychological stress detection and early warning system is examined in detail. In Section 3, the experimental environment and results are discussed. Finally, the paper is concluded in Section 4.

2. Psychological Stress Detection and Early Warning System

In this section, first we discuss the design of our system hardware platform that was required to conduct this study. Next, we discuss the system software design and proposed methodology of this paper.

2.1. System Hardware Design. The hardware of psychological stress detection and early warning system mainly includes pulse acquisition module, signal low-pass filtering and amplification module, real-time clock module, wireless network transmission module, and power supply module, respectively.

2.1.1. Pulse Acquisition Module. To realize accurate collection of pulse signal, SC0073B micro-dynamic pulse micropressure sensor is used [8]. It is a miniaturized piezoelectric sensor, which uses the electric film as the energy exchange material. The pulse pulsates and presses the film of the pulse sensor to produce the output of charge. The sensor has the physical characteristics of simple operation: its small volume and lightweight and low-cost features. Its advantages are high sensitivity coefficient, strong resistance to overload and shock waves, and good resistance to external interference. The application circuit design of SC0073B pulse sensor is simple. It only needs to be connected in series with a 10 K resistor. The circuit structure of pulse acquisition module is shown in Figure 1.

2.1.2. Signal Low-Pass Filtering and Amplification Module. Because the SC0073 B pulse sensor is very sensitive, the external high-frequency disturbance greatly interferes with the pulse signal. Hence, this paper adds a low-pass filter circuit to the hardware system [9]. The additional high-frequency disturbance signals can be filtered out by effective RC combination. The pulse signal frequency range is from 0.8 Hz to 10 Hz, so the upper limit cutoff frequency of the low-pass filter is 25 Hz. Thus, the following equation exists:

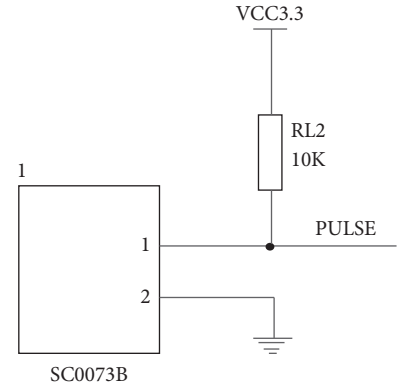

Figure 1: Circuitry of the pulse acquisition module.

$$f = \frac{1}{2\pi RC}. \tag{1}$$

It can be observed that the upper limit cutoff frequency of RC low-pass filter is related to the values of R and C. In (1), $f = 25\,Hz$ and C is fixed at $0.1uf$; thus,

$$R = \frac{1}{2\pi Cf}. \tag{2}$$

If $R \approx 637\,\Omega$ and the nominal value of the nearest resistance is 620, then the upper limit cutoff frequency is 25.6 Hz, which meets the design requirements. The low-pass filtering circuit is shown in Figure 2.

The output signal amplitude of SC0073B pulse sensor is nearly 200 mV. In order to improve the AD sampling accuracy of embedded processor, this paper adopts AD623 high-precision differential amplifier to amplify and process the pulse signal [10].

The AD623 has a high input impedance, a low output impedance, and a high common mode rejection ratio and can achieve small signal amplification from 1 to 1000 times via an external gain resistor. AD623 can be dual power supply or single power supply and has a zero adjustment circuit interface through the external potentiometer adjustment. These features realize the balance output of zero adjustment. The system in this paper adopts 3.3 V embedded processor, so the input voltage range of AD interface is 0 to 3.3 V. Therefore, in this paper, the output signal of the pulse sensor was amplified by 10 times [11], and the gain resistance of AD623 was calculated using

$$V_o = \left[1 + \frac{100K\Omega}{R_G}\right] V_i. \tag{3}$$

Here, $R_G \approx 11K$. The AD623 amplifier circuit is shown in Figure 3.

In Figure 3, RL1, RL6, RL7, and RL4 constitute the balance bridge circuit, whereas CL1, CL2, and CL3 constitute the input filter circuit.

2.1.3. Real-Time Clock Module. The psychological stress detection and early warning system, designed in this paper, need to record the real pulse sampling interval. For this

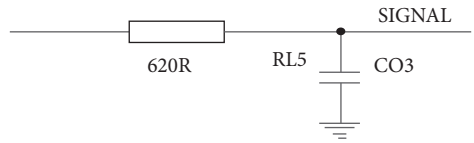

Figure 2: Circuitry of low-pass filtering.

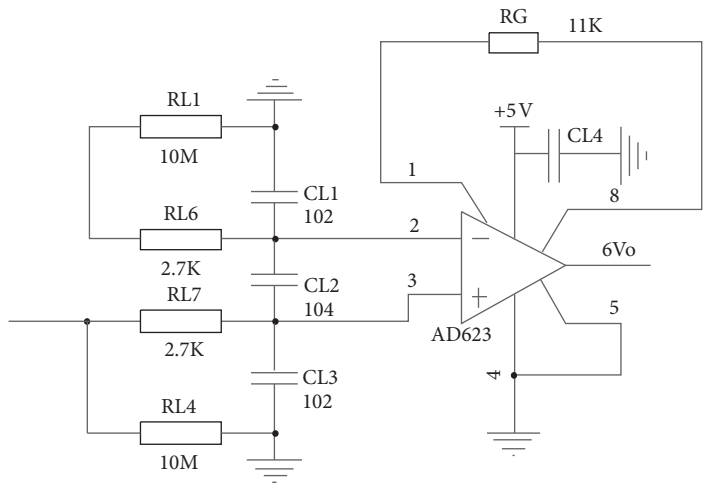

Figure 3: Enlarged circuit diagram of AD623.

purpose, the real-time clock module needs to be designed [12]. The real-time clock chip model is RX6110, which has a built-in oscillator and integrated calendar function, and uses I2C bus to communicate with MCU. The circuit configuration is relatively simple, as shown in Figure 4.

It should be noted that the clock chip needs at least 40 ms startup time when it is powered on, and registers in the chip cannot be read or written before the startup is completed.

2.1.4. Wireless Transmission Module. The collected pulse signal eventually needs to be uploaded to a PC for processing. This system uses CP2102 chip to realize UART/USB conversion. The circuitry of wireless network transmission module is shown in Figure 5.

The serial communication rate is set at 115200 bps, there is no parity check, and one stop bit is used. In addition to the communication function, CP2102 also integrates 3 V LDO, which can stabilize the input voltage of 5 V to 3 V and directly output to the processor.

2.1.5. Power Supply Module. This system is powered by USB and lithium rechargeable battery, and the circuit is shown in Figure 6.

When the power supply is connected to USB, it is powered by USB interface that charges the rechargeable battery. In this case, the charging current is slightly less than 1 A. When the USB interface is disconnected, it is automatically powered by a rechargeable battery. The processor can easily identify the USB connection status and charging status and can sense the charging battery voltage. In practical tests, the 2000 mAh battery provides the system with at least 50 hours of continuous operation on a full charge.

2.2. System Software Design. Pulse is an important physiological signal of human body, which is well known and has rich clinical experience. The continuous periodic contraction and diastole of the heart cause blood to flow from the aortic root along the arterial system, and vascular pressure is generated during the blood flow. The response of pressure wave generated by the change of vascular pressure and blood flow on the body surface can be called pulse [13]. Under normal circumstances, the pulse signal is continuous, close to cyclical deterministic signal. The pulse of different individuals in different states is not identical. Under normal circumstances, a person's pulse frequency is 60 to 100 times/min. The pulse signal is, in fact, not certain, so the pulse signal is not stable and changes periodically. It changes with the changes of various physiological and psychological factors of the human body and the external environment, and the waveform obtained through instruments and equipment will also change accordingly [14]. Pulse signals have the following characteristics:

(i) It is vulnerable to external interference and has the characteristics of small amplitude. Because pulse signals originate from the surface of the human body and ranges from 10 V to 100 V, they are highly susceptible to interference by EMG signals, electronic devices, and mental stress.

(ii) Pulse signal beats about 1 to 10 times per second, which is a typical low-frequency signal. The pulse frequency of normal healthy human body is 1–5 Hz, and the pulse frequency may exceed this range in some healthy cases [15]. In general, the distribution of pulse frequency will be less than 1 Hz or more than 5 Hz when human lesions occur.

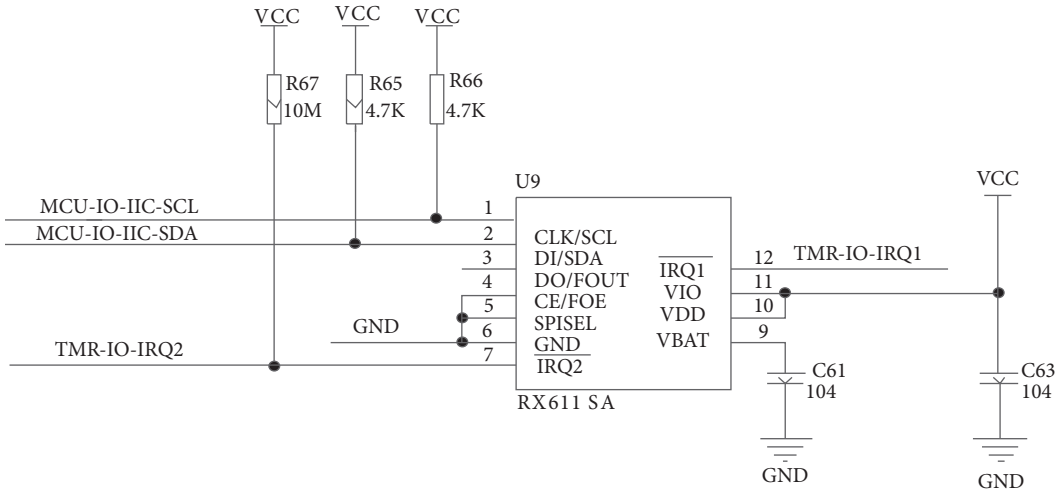

Figure 4: Real-time clock circuitry.

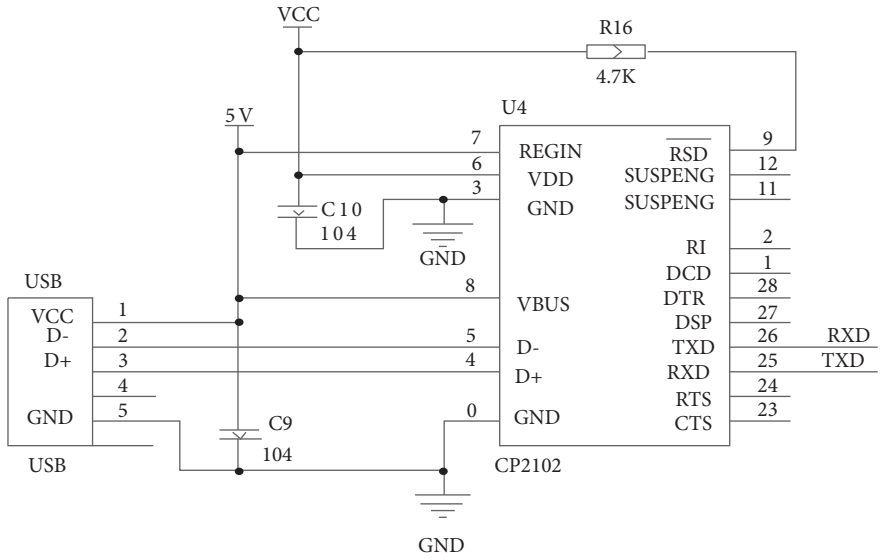

Figure 5: Wireless network transmission module circuitry.

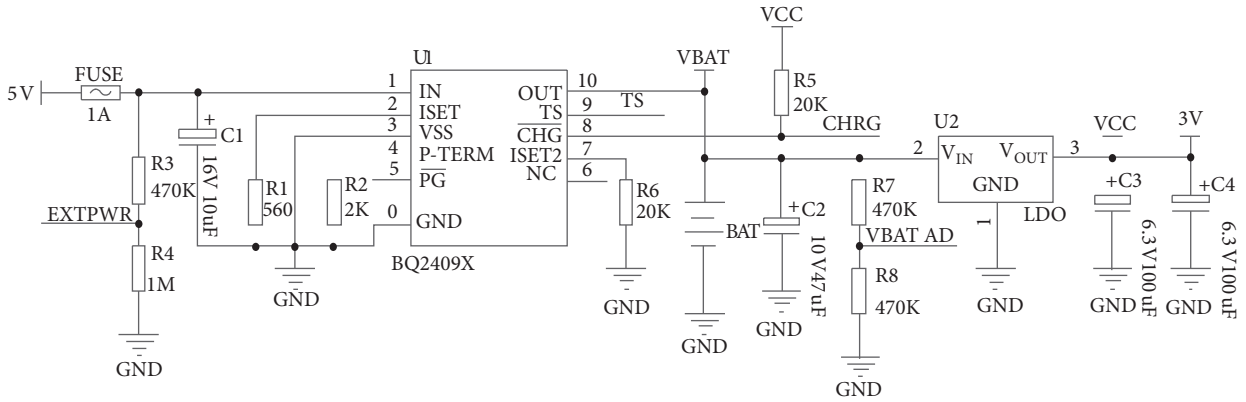

Figure 6: Power supply circuitry.

(iii) It has the characteristics of volatility and instability and changes with the changes of various physiological and psychological factors of the human body and the external environment, presenting different pulse conditions. Because of the complexity and uncertainty of pulse detection, it is nearly impossible to directly analyze and summarize its characteristics from pulse signals. Hence, it is impossible to determine whether some signals are meaningful or not.

In this paper, if the signal is denoted by $s(n)$, then the pulse signal's noise model in the actual environment can be simplified using

$$s(n) = f(n) + \sigma \cdot e(n), \tag{4}$$

where $f(n)$ is pure signal, $e(n)$ is noise, and σ is the noise intensity. In simple case, $e(n)$ is Gaussian white noise and $\sigma = 1$.

The wavelet's packet structure is used to decompose the perceptual wavelet packet of noisy speech signal, and multiple wavelet subbands are obtained using

$$w_j(k) = \mathrm{PWPD}\{x(n)\}, \tag{5}$$

where $w_j(k)$ represents the wavelet coefficient in the subband $j = (1, 2, \ldots, n)$ and k is the sequence number of the wavelet coefficient.

The improved Teager energy operator (TEO) coefficient is calculated by using (6), which is described as follows:

$$t_j(k) = E'\left[w_j(k)\right]. \tag{6}$$

Among them,

$$E_n = \frac{\left(3x_n^2 - 4x_{n-1}x_{n+1} + x_{n-2}x_{n+2}\right)}{3}. \tag{7}$$

A second-order low-pass IIR filter is used to smooth the TEO coefficients, and a mask $M_j(k)$ is obtained. Through low-pass filtering operation, the voiceless component in the speech signal can be well protected using

$$M_j(k) = t_j(k) \cdot h_j(k), \tag{8}$$

where $h_j(k)$ represents the smoothing coefficient.

The compensation value S_j is found from the distribution function using

$$S_j = \mathrm{abscissa}\left[\max\left(H\left(M_j(k)\right)\right)\right]. \tag{9}$$

A new mask is obtained by processing the above results. The compensation value is the maximum distribution of the mask values. The results are as follows:

$$M_j'(k) = \left[\frac{M_j(k) - S_j}{\max\left(M_j(k) - S_j\right)}\right]^{1/8}. \tag{10}$$

Next, divide the subbands into different parts and calculate the variance of each part. The result is as follows:

$$w_{j,m}'(k_m) = \mathrm{Split}\left[w_j(k)\right], \tag{11}$$

where $w_{j,m}'(k_m)$ is the wavelet coefficient of the m^{th} part of the j^{th} subband and k_m is the sequence number of the wavelet coefficient after frame splitting. The proportionality coefficient is defined as

$$\beta_{j,m}\frac{\min\left[\mathrm{var}\left(w_{j,m}'(k_m)\right)\right]}{\mathrm{var}\left(w_{j,m}'(k_m)\right)}. \tag{12}$$

For a given subband j, its adaptive threshold is defined as

$$\lambda_j'(k) = \beta_{j,m} \cdot \lambda_j\left(1 - M_j'(k)\right), \tag{13}$$

where λ_j represents the fixed thresholds of different subbands and is calculated using

$$\lambda_j = \sigma_j\sqrt{2\ \log\left(N\ \log_2\ N\right)}. \tag{14}$$

In (14), σ_j represents the noise intensity of subband j and N represents the number of subbands.

In this paper, adaptive threshold is used to conduct soft threshold processing for each subband coefficient, and its processing is highlighted using (13).

$$\widehat{w}_j(k) = \begin{cases} 0, & \left|w_j(k)\right| \le \lambda_a, \\ \mathrm{sgn}\left(w_j(k)\right)\left(\left|w_j(k)\right| - \lambda_a\right), & \left|w_j(k)\right| > \lambda_a, \end{cases} \tag{15}$$

where λ_a represents the wavelet denoising threshold and is calculated using

$$\lambda_a = \begin{cases} \lambda_j', & S_j \le 0.35\max\left(M_j(k)\right), \\ \lambda_j, & S_j > 0.35\max\left(M_j(k)\right). \end{cases} \tag{16}$$

According to the processed coefficients, the inverse wavelet packet transform of perception is carried out to obtain the reconstructed signal:

$$\widehat{x}(n) = \mathrm{PWPD}^{-1}\left\{\widehat{w}_j(k)\right\}. \tag{17}$$

According to the sample data, the basic analysis found that although the shape of each pulse signal waveform is not exactly the same, but each pulse waveform of the distribution and morphological characteristics of peaks and troughs are almost constant. Moreover, the pulse signal acquisition and pressure curve's turning point positioning is the pulse signal eigenvalue extraction. At the same time, there are several turning points in a pulse signal, which shows that the extreme value point of the basic characteristics of pulse signal waveform is stable. The extraction algorithm based on the peak of the pulse signal was analyzed along with the positioning of the pulse of a few key extremum points. The analysis of extreme value point of properties ensures to get the maximum and minimum values. Thus, a pulse waveform is quantitatively calculated and the physiological information contained in the value is analyzed. Figure 7 is the basic flow chart of the complete waveform detected by the extreme point of the pulse signal based on the peak value.

The basic description of the complete waveform of pulse signal's extremum point detection as shown in Figure 7 is as

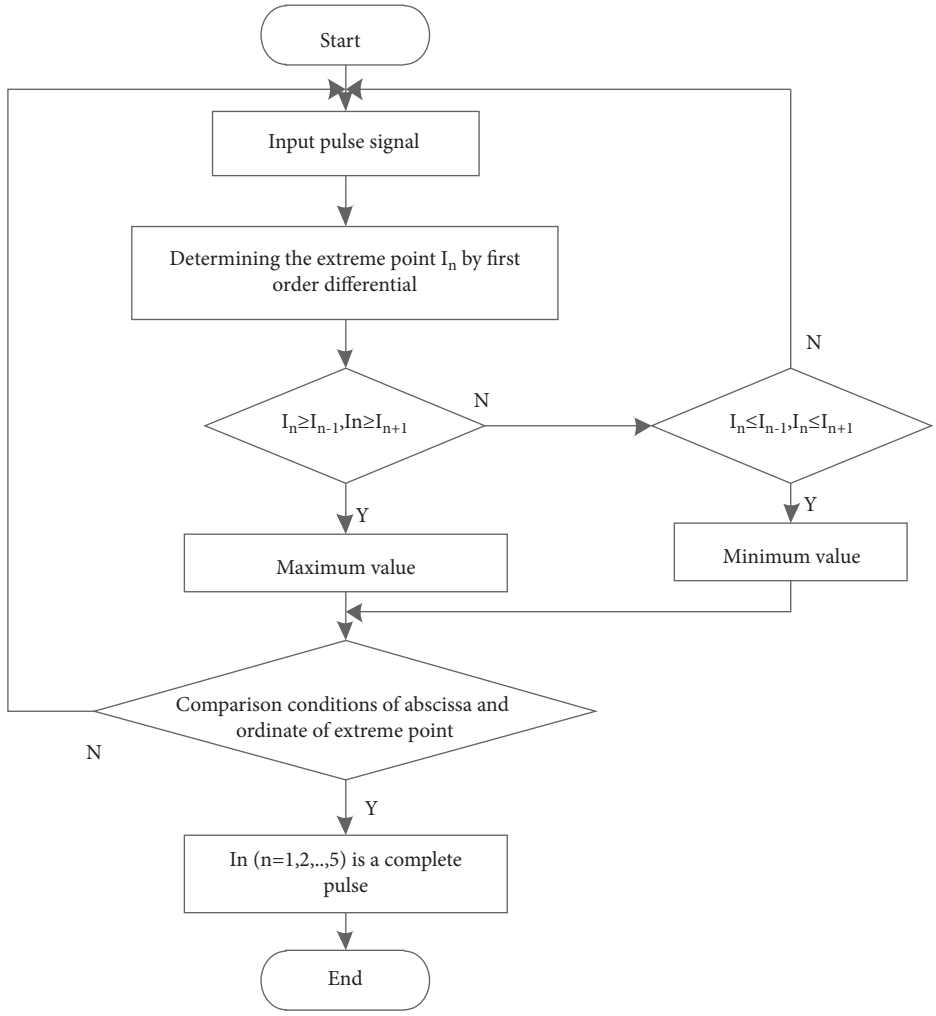

Figure 7: Flowchart for waveform detection.

follows: after the pulse signal is filtered, it enters the detection program, the extremum point of pulse signal is determined through first-order differential, and the amplitude of several adjacent extremum points is compared and determined.

For the first five adjacent extreme points I_1, I_2, I_3, I_4, and I_5 if

(i) I_1, I_3, I_5 are local minima, and $Y_{11} < Y_{13}$, $Y_{11} < Y_{13}$, (Y_i is the y-coordinate of I)

(ii) I_2 and I_4 are local maxima, and $Y_{12} > Y_{14}$

(iii) $Y_{12} > Y_{11}$ and $Y_{12} > Y_{13}$

(iv) $Y_{14} > Y_{13}$ and $Y_{14} > Y_{15}$

(v) $X_{15} - X_{14} > X_{12} - X_{11}$ (X_i is the abscissa of point I)

The above statements show that I_1, I_2, I_3, I_4, and I_5 locate a complete pulse. If these five requirements/statements are not met, the first point I_1 is discarded and the sixth extreme point I_6 is added. The five new extreme point sequences I_1, I_2, I_3, I_4, and I_5 are taken as the new sequence to judge whether the above conditions are met by moving the panes one by one to be determined. If all of the above five points are met, then they are determined to locate a complete pulse. In the next judgment, these five points should be discarded and the next five extreme points should be added to repeat the above judgment. If successful, Step 5 uses units of extreme point to judge the feature points.

According to the determination of the peak point, after extracting the characteristic value and obtaining the complete pulse, we can accurately calculate the subamplitude, heartbeat interval, the amplitude of the repeat pulse, the first and second peak interval, etc., i.e., the number of complete pulse, pulse amplitude (PPGA), and heartbeat interval (HBI).

The original data of pulse amplitude and state interval need to be normalized through normalization calculation. Linear normalization algorithm is used to normalize the data from 0 to 1 using

$$\text{norm} = \frac{(\text{data} - \min)}{(\max - \min)}. \tag{18}$$

Psychological stress index is widely used in the operation process to monitor the pain of patients during the operation. The more the surgical pressure index value approaches 100,

Table 1: Experimental environment.

Experimental environment	Configuration	Parameter
Hardware environment	CPU	Intel(R)Core(TM)i5-9400
	Frequency	2.90 GHz
	RAM	16.0 GB
Software environment	Operating system	Windows 10
	Version	18362.1082 pro
	Digits	64 bit
	Analog software language	APDL

the higher the stress level of the patient is. The more the index value approaches 0, the lower the stress level of the patient is. In order to effectively carry out the psychological stress test, the psychological stress index (PSI) is proposed to quantify the degree of psychological stress. The equation of the psychological stress index is as follows:

$$\mathrm{PSI} = 100 \times (1 - J \times \mathrm{PPGAnorm} - (1 - J) \times \mathrm{HBInorm}). \tag{19}$$

According to the above analysis, a threshold value is set. When the PSI $\geq T$, the subject is considered to be under too much psychological pressure. At this time, the system should be used for early warning, so as to further reduce people's psychological pressure and improve people's mental health level through relevant intervention means.

3. Experimental Setting and Result Analysis

In this section, the experimental setup is provided in Section 3.1. The comprehensive analysis and discussion of various experimental results are discussed in Section 3.2.

3.1. Experimental Settings. In order to verify the practical application of the psychological stress detection and early warning system based on wireless network transmission, experimental analysis is needed. For this purpose, an experimental environment needs to be setup, as shown in Table 1.

Pulse signal is collected according to the above experimental settings, and the specific environment is shown in Figure 8.

To measure the effectiveness of stress detection and warning system, it is necessary to set up the experimental paradigm of inducing psychological stress. Research approaches of psychological pressure identification have special circumstances, special groups, and experimental excitation. The expectations of crowd recognition add to the natural pressure, although the authenticity and validity are better. Stress tasks in experimental environment can stimulate certain psychological stress and cause changes in physiological signals. Most of these tasks stimulate psychological stress through experiments. These tasks are mainly used in public speaking and language interaction, cognition, emotional elicitation, noise exposure tasks, etc.

Proactive tasks require the subjects to make timely cognitive responses, such as public speaking and mental arithmetic. Social evaluation factors generally include permanent record of personal performance through audio tapes or video cameras. At least one member of the audience takes part in the test subject's task. In this study, different subjects were compared. Since proactive task and social evaluation are more capable of causing significant physiological responses, this study adopted proactive stress task combined with speech and cognitive task, which is described as follows:

(i) Proactive task: the subject is required to make a speech and discussion on stage in nonnative English

(ii) There is a time limit for the speech process, which is set at 10 minutes

(iii) Give a speech to two experts and engage in discussion with them

(iv) Let two subjects give a speech in adjacent places at the same time, and the subjects know the process

3.2. Analysis of Experimental Results. In order to verify the effectiveness of the system designed in this paper, the psychological stress of 1000 subjects was tested, and the test results were compared with the expert results. Among them, the subjects' mental health test results were scored by several psychological experts to take the average of the final results. The comparison results for the first 20 subjects are shown in Table 2.

The analysis of the data in Table 2 shows that the psychological stress test results obtained in this paper are basically consistent with the expert evaluation results. The remaining 980 subjects were tested, and the results were basically consistent with the expert evaluation results. These results can realize the psychological pressure and high precision detection. According to the above results, in the 1000 subjects, more than half of the subjects' psychological stress exceeds the threshold value, so the psychological stress warning time will be tested. Since the early warning time of psychological stress is also one of the important indicators to verify the psychological stress detection and early warning system, the subjects whose psychological stress threshold exceeds the threshold are selected for the psychological stress early warning time test, and the results are shown in Figure 9.

According to the data in Figure 9, the warning time of the system designed in this paper varies between 0.11 s and 0.64 s in the process of warning for 500 subjects whose psychological stress exceeds the threshold. This indicates

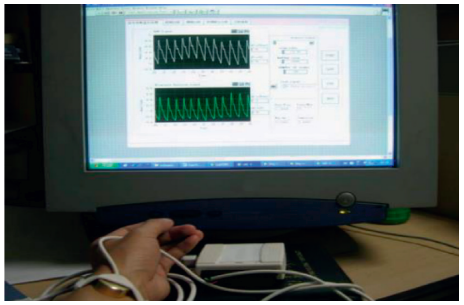

Figure 8: Experimental environment for pulse signal acquisition.

Table 2: Comparison of psychological stress test results.

Subject number	Expert rating	The system test results presented in this paper
1	56	57
2	23	23
3	35	36
4	86	85
5	75	76
6	21	22
7	28	28
8	41	40
9	36	36
10	66	67
11	35	34
12	87	88
13	74	74
14	83	85
15	56	56
16	42	41
17	33	33
18	80	78
19	74	71
20	46	46

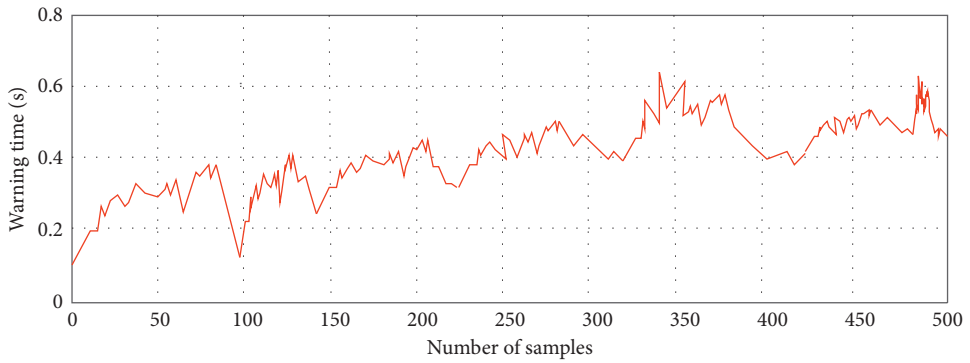

Figure 9: Psychological stress warning time test results.

that the warning time of this system for psychological stress is short and the warning efficiency is high, which can be further promoted in practice.

4. Conclusion

In modern society, people are exposed to all kinds of stress. They often need to work under pressure that affects their life, interpersonal relationship, and various other aspects. Persistent stress can bring mental and physical obstacles and defects, so the prevention, diagnosis, and treatment of psychological stress have received extensive attention from all walks of life, especially in the medical field. This paper designed psychological stress detection and early warning system based on wireless network transmission and proposed system development through the system hardware and software design. Experimental results show that psychological stress test results are almost consistent with expert

evaluation results, and the warning time is shorter. Furthermore, the proposed system has high psychological pressure detection accuracy and low detection time. In practice, it can further promote and lay a solid foundation for modern people to alleviate psychological pressure.

Data Availability

The data used to support the findings of this study are available from the corresponding author upon request.

Conflicts of Interest

The author declares that there are no conflicts of interest.

Acknowledgments

This study was supported by the Guangdong Province 2018 Education Science "13TH FIVE-YEAR PLAN" Project: A Study on the Liberal Education Model of College Students Psychological Development Based on the Cultivation of Applied Talents (2018GXJK167).

References

[1] X. Sheng, Y. Wang, W. Hong, Z. Zhu, and X. Zhang, "The curvilinear relationship between daily time pressure and work engagement: the role of psychological capital and sleep," *International Journal of Stress Management*, vol. 26, no. 1, pp. 25–35, 2019.

[2] M. Kassis, S. L. Schmidt, D. Schreyer, and M. Sutter, "Psychological pressure and the right to determine the moves in dynamic tournaments-Evidence from a natural field experiment," *CREMA Working Paper Series*, vol. 126, no. 1, pp. 278–287, 2020.

[3] H.-L. Zhang, R. Jin, Y. Zhang, and Z. Tian, "A public psychological pressure index for social networks," *IEEE Access*, vol. 8, no. 1, Article ID 23457, 2020.

[4] J. Q. Zhong, L. F. Huang, W. U. Zhi et al., "Survey on the university medical students' cognition and psychological pressure of standardized training system for specialist physicians," *Medical Education Research and Practice*, vol. 27, no. 4, pp. 611–614, 2019.

[5] A. Ciarlone and G. Trebechi, "Designing an early warning system for debt crises," *Emerging Markets Review*, vol. 6, no. 4, pp. 376–395, 2005.

[6] R. L. Luan, M. X. Zhu, and H. Y. Sun, "Effect of comprehensive nursing intervention in preventing postoperative pain, complications, and psychological pressure in the otolaryngology department," *Medicine*, vol. 98, no. 24, Article ID e15923, 2019.

[7] M. Nishimura, M. Suzuki, R. Takahashi et al., "Daily ingestion of eggplant powder improves blood pressure and psychological state in stressed individuals: a randomized placebo-controlled study," *Nutrients*, vol. 11, no. 11, pp. 2797–2786, 2019.

[8] A. Van de ndriessche, A. Ghekiere, C. Van et al., "Does sleep mediate the association between school pressure, physical activity, screen time, and psychological symptoms in early adolescents? A 12-country study," *International Journal of Environmental Research and Public Health*, vol. 16, no. 6, pp. 1–12, 2019.

[9] F. Wan, Z. Yuan, B. Ravelo, J. Ge, and W. Rahajandraibe, "Low-pass NGD voice signal sensoring with passive circuit," *IEEE Sensors Journal*, vol. 20, no. 99, pp. 1–10, 2020.

[10] D. Vercaemer, J. Raman, and P. Rombouts, "Low-pass filtering SC-dac for reduced jitter and slewing requirements on CTSDMs," *IEEE Transactions on Circuits and Systems I: Regular Papers*, vol. 66, no. 4, pp. 1369–1381, 2019.

[11] C. Qi, J. He, L.-H. Fu et al., "Tumor-specific activatable nanocarriers with gas-generation and signal amplification capabilities for tumor theranostics," *ACS Nano*, vol. 15, no. 1, pp. 1627–1639, 2020.

[12] T. . Han, "Fractal behavior of BDS-2 satellite clock offsets and its application to real-time clock offsets prediction," *GPS Solutions*, vol. 24, no. 2, pp. 1–12, 2020.

[13] E. L. Foltz, J. P. Blanks, and K. Yonemura, "CSF pulsatility in hydrocephalus: respiratory effect on pulse wave slope as an indicator of intracranial compliance," *Neurological Research*, vol. 12, no. 2, pp. 67–74, 2019.

[14] K. Sonnabend, G. Brinker, D. Maintz, A. C. Bunck, and K. Weiss, "Cerebrospinal fluid pulse wave velocity measurements: in vitro and in vivo evaluation of a novel multiband cine phase ontrast MRI sequence," *Magnetic Resonance in Medicine*, vol. 85, no. 1, pp. 1–10, 2020.

[15] A. Gloria, L. Di Francesco, G. Marruchella, D. Robbe, and A. Contri, "Pulse-wave Doppler pulsatility and resistive indexes of the testicular artery increase in canine testis with abnormal spermatogenesis," *Theriogenology*, vol. 158, no. 1, pp. 454–460, 2020.